AIP | Journal of Applied Physics

Plasma-oxidation of Ge(100) surfaces using dielectric barrier discharge investigated by metastable induced electron spectroscopy, ultraviolet photoelectron spectroscopy, and x-ray photoelectron spectroscopy

L. Wegewitz, S. Dahle, O. Höfft, F. Voigts, W. Viöl et al.

Citation: J. Appl. Phys. **110**, 033302 (2011); doi: 10.1063/1.3611416
View online: http://dx.doi.org/10.1063/1.3611416
View Table of Contents: http://jap.aip.org/resource/1/JAPIAU/v110/i3
Published by the American Institute of Physics.

Plasma-oxidation of Ge(100) surfaces using dielectric barrier discharge investigated by metastable induced electron spectroscopy, ultraviolet photoelectron spectroscopy, and x-ray photoelectron spectroscopy

L. Wegewitz,[1] S. Dahle,[1,2] O. Höfft,[3] F. Voigts,[2,3] W. Viöl,[4] F. Endres,[3] and W. Maus-Friedrichs[1,2,a)]

[1]*Clausthaler Zentrum für Materialtechnik, Technische Universität Clausthal, Leibnizstrasse 4, 38678 Clausthal-Zellerfeld, Germany*
[2]*Institut für Physik und Physikalische Technologien, Technische Universität Clausthal, Leibnizstrasse 4, 38678 Clausthal-Zellerfeld, Germany*
[3]*Institut für Mechanische Verfahrenstechnik, Technische Universität Clausthal, Arnold-Sommerfeld-Strasse 6, 38678 Clausthal-Zellerfeld, Germany*
[4]*Hochschule für Angewandte Wissenschaft und Kunst, Fakultät für Naturwissenschaften und Technik, Von-Ossietzky-Straße 99, 37085 Göttingen, Germany*

(Received 31 January 2011; accepted 18 June 2011; published online 2 August 2011)

The radical oxidation of Ge(100) applying a dielectric barrier discharge plasma was investigated using metastable induced electron spectroscopy, ultraviolet photoelectron spectroscopy, and x-ray photoelectron spectroscopy. The plasma treatments were performed in a pure oxygen atmosphere as well as under environmental conditions at room temperature. In both atmospheres GeO_2 layers up to thicknesses of several nm were formed on the Ge(100) surface. © *2011 American Institute of Physics*. [doi:10.1063/1.3611416]

I. INTRODUCTION

Germanium is a promising candidate for applications in MOSFET gate oxides mainly because of its higher electron and hole mobility and its lower tunneling currents compared to SiO_2 of equal thickness. Furthermore, Ge is compatible to standard Si MOS technologies mainly due to its lower melting temperature compared to Si.[1–3] Therefore, GeO_2 is principally well suited as MOSFET gate oxide material.

Unfortunately, GeO_2 is thermally not as stable as SiO_2. At temperatures beyond 420 °C, GeO_2 decomposes desorbing GeO.[1,4] Furthermore GeO_2 is hygroscopic and soluble in water.[1,2] This makes it necessary to avoid any contact to H_2O molecules during the oxide formation and to develop low temperature or high oxygen pressure procedures for GeO_2 formation.

The oxidation of Ge (100) and Ge(111) surfaces was studied previously in detail under high vacuum conditions, applying surface physics techniques such as auger electron spectroscopy, x-ray photoelectron spectroscopy (XPS), ultraviolet photoelectron spectroscopy (UPS), scanning tunneling spectroscopy, scanning tunneling microscopy, and high resolution electron energy loss spectroscopy supported by density functional theory calculations.[5–14] The initial sticking coefficient for oxygen is found between 10^{-3} and 10^{-2} for most Ge surfaces at room temperature.[9,15] This is at least ten times lower than the initial oxygen sticking coefficient on Si(100) and Si(111), which is found to be around 10^{-1}.[15,16] In contrast to the plasma-oxidation, the oxidation out of an oxygen containing atmosphere starts at specific surface defects and not at domain boundaries.[7] Roughening of the surface for example by moderate sputtering with Ar^+ ions increases the initial oxidation rate.[14] This means that the dissociation of impinging oxygen molecules is most likely only possible at such surface defects. The oxidation then proceeds by the reaction with surrounding Ge atoms forming oxidized islands at these defect sites.[7] On Ge(100) 2×1 surfaces, the most stable initial structure consists of one oxygen atom in the Ge dimer backbond and another oxygen atom in the dimer bridge between the Ge atoms.[13] The activation energy for bridging atoms to be underneath the Ge surface is calculated to about 0.8 eV, which makes the formation of thicker oxide films at room temperature very unlikely. Oxidation of germanium surfaces under ambient conditions yields thin GeO_2 films with thicknesses between 0.6 and 0.8 nm after several days of exposure.[17] This means that after the initial saturation of surface defects by the oxidation, the dissociation probability of further impinging O_2 molecules decreases and reaches zero when the top layer oxidation is completed. Only a few studies apply metastable induced electron spectroscopy (MIES) to Ge and Ge oxides.[18,19] These will be discussed together with our own results in Sec. III.

As described above, the oxidation at room temperature does only lead to thin GeO_2 layers which contain impurities and Ge in different oxidation states. The formation of sufficiently thick and well defined GeO_2 layers therefore requires other procedures.

During the direct thermal oxide formation, Ge surfaces are heated between 450 and 600 °C in an oxygen atmosphere of typically 1000 hPa. At this pressure any GeO_2 decomposition is avoided.[20,21] At 250 °C a Ge oxide layer only grows to a thickness of about 4 monolayers even for a duration of 300 min in an atmosphere of 0.5 bar.[22] The formation of thicker oxide films is only observed for temperatures below 450 °C because the activation energy amounts to about

a)Author to whom correspondence should be addressed. Electronic mail: w.maus-friedrichs@pe.tu-clausthal.de.

1.7 eV.[2] Cracium *et al*. found oxide growth already at temperatures below 450 °C but the oxidation was supported by VUV radiation at 172 nm.[23] The thermal oxidation at 450 °C leads to the formation of mainly GeO_2. The film formation and the GeO_2/Ge interface structure are the same for the surface orientations Ge(100), (110), and (111).[24]

Another possibility for oxide formation is the growth of GeO_2 layers by atomic layer deposition typically at temperatures between 350 and 450 °C in an oxygen atmosphere.[1,4]

All procedures described so far deliver well defined GeO_2 layers grown up to sufficient thicknesses and very low interface defect densities. Furthermore, each of these thermal oxidation procedures requires a complex surface pretreatment consisting of various chemical etching and annealing steps.

During plasma-enhanced oxidation, radical oxygen atoms are produced within the plasma which forms GeO_2 on top of Ge surfaces up to sufficiently high thickness.[2,3] In contrast to room temperature or thermal oxidation the oxygen molecule dissociation, which is the first step in any oxygen-surface interaction, must not be performed by the surface itself.[25] This is the rate limiting step in most oxidation processes. Usually slot-plane antennas are applied for the oxidation, see Ref. 2 for a detailed description. Ge wafers are cleaned from organic contaminants by a mild O_2 plasma stream and then by repeated chemical etching steps with HF and HCl. Afterwards the plasma oxidation starts building up GeO_2 oxide layers on Ge wafers. In contrast to the thermal oxidation, the activation energy is only about 0.23 eV and temperatures between 300 and 350 °C are sufficient for the oxidation.[2,26]

All these technological relevant oxidation procedures need elevated temperatures and sophisticated cleaning procedures. In opposition to these ambitious techniques we provide an alternative method for the Ge oxidation applying a dielectric barrier discharge (DBD) plasma operating at room temperature. XPS is used for the analysis of the chemical composition of Ge and Ge oxides as well as for the investigation of the oxide thicknesses. The combination of MIES and UPS is applied for the investigation of the surface compositions. We will demonstrate that GeO_2 films of thicknesses up to several nm grow very well by the use of a DBD plasma treatment in an oxygen atmosphere. Furthermore, we will show that even in ambient atmospheric conditions GeO_2 layers of high quality are formed.

II. EXPERIMENTAL

An ultra high vacuum apparatus with a base pressure of 5×10^{-11} hPa, which has been described in detail in a preceding study,[27] is used to carry out the experiments. All measurements were performed at room temperature.

Electron spectroscopy is performed using a hemispherical analyzer (VSW HA100) in combination with a source for metastable helium atoms (mainly He* $^3S_1$) and ultraviolet photons (HeI line). A commercial non-monochromatic x-ray source (Specs RQ20/38 C) is utilized for XPS.

During XPS, x-ray photons hit the surface under an angle of 80° to the surface normal, illuminating a spot of several mm in diameter. The Al K_α line with a photon energy of 1486.6 eV is used for all measurements presented here. Electrons are detected by the hemispherical analyzer with an energy resolution of 1.1 eV under an angle of 10° to the surface normal. All XPS spectra are displayed as a function of binding energy with respect to the Fermi level.

For quantitative XPS analysis, photoelectron peak areas are calculated via mathematical fitting with Gauss-type profiles using OriginPro 7G including the PFM fitting module, which applies Levenberg–Marquardt algorithms to achieve the best agreement between experimental data and fit. To optimize our fitting procedure, Voigt-profiles have been applied to various oxidic and metallic systems but for most systems the Lorentzian contribution converges to 0. Therefore all XPS peaks are fitted with Gaussian shapes. Photoelectric cross sections as calculated by Scofield[28] with asymmetry factors after Refs. 29, 30 and inelastic mean free paths from the NIST database[31] (using the dataset of Tanuma, Powell, and Penn for elemental Ge and the TPP-2M equation for GeO_2) as well as the energy dependent transmission function of our hemispherical analyzer are taken into account when calculating stoichiometry.

MIES and UPS are performed applying a cold cathode gas discharge via a two-stage pumping system. A time-of-flight technique is employed to separate He* atoms (for MIES) from HeI photons (for UPS). Electrons emitted by He* interaction with the surface and photoelectrons are detected alternately at a frequency of 2000 Hz. Thus, both spectra are recorded quasi simultaneously. The recording of such a MIES/UPS spectrum requires 280 seconds. The combined He*/HeI beam strikes the sample surface under an angle of 45° to the surface normal and illuminates a spot of approximately 2 mm in diameter. The spectra are recorded by the hemispherical analyzer with an energy resolution of 220 meV under normal emission.

MIES is an extremely surface sensitive technique probing solely the outermost layer of the sample, because the He* atoms interact with the surface typically 0.3 to 0.5 nm in front of it. This may occur via a number of different mechanisms depending on surface electronic structure and work function, as described in detail in other publications.[32–34] Only the processes relevant for the spectra presented here shall be discussed shortly.

During Auger deexcitation (AD) an electron from the sample fills the 1s orbital of the impinging He*. Simultaneously, the He 2s electron carrying the excess energy is emitted. The resulting spectra reflect the surface density of states (SDOS) directly. AD-MIES and UPS can be compared and allow a distinction between surface and bulk effects. AD takes place for oxide surfaces and metal or semiconductor surfaces with work functions below about 3.5 eV.

The Auger neutralization process (AN) occurs at pure metal or semiconductor surfaces with work functions beyond 3.5 eV.[35,36] Hereby the impinging He* atom is ionized by a resonant transfer of its 2s electron into unoccupied surface states beyond the Fermi level. Afterwards, the remaining He^+ ion is neutralized by a surface electron thus emitting a second surface electron carrying the excess energy. The observed electron spectrum is rather structureless and originates from a self convolution of the surface density of states.

All MIES and UPS data have been corrected for the analyzer transmission function, that is proportional to E^{-1} in this energy range. The spectra are displayed as a function of the electron binding energy with respect to the Fermi level. The surface work function can be determined from the high binding energy onset of the MIES or the UPS spectra with an accuracy of ± 0.1 eV.

Ge(100) surfaces were cleaned with the chemical rinsing method introduced by Prabhakaran *et al.*[25] Initially, the sample is washed in de-ionized water, this will be repeated after each of the following steps. Then the sample is etched in HF (48%) for 15 s. Subsequently, chemical oxidation by dipping in H_2O_2 (30%) for 15 s is performed. This procedure is repeated 5 times thereby forming a thin oxide layer in the last step before drying the sample in a nitrogen gas flow and transferring it into the UHV chamber. Finally the sample is annealed at 300 °C for 30 min and further heated to 500 °C (15 min) for desorption of the oxide film grown earlier in the process. All samples cleaned by this technique are referred to as "clean Ge(100)" below. We applied this procedure to allow a comparison of our data with the literature.

All plasma treatments are carried out in a preparation chamber with a base pressure of 5×10^{-8} hPa which is connected directly to the UHV recipient via a common transfer system. The chamber is equipped with an electrode for the dielectric barrier discharge and the sample is mounted on a manipulator for precise positioning in front of the electrode. O_2 (Linde Gas, 99.995%) or the ambient atmospheric air is offered via backfilling the chamber using a bakeable leak valve. The gas line is evacuated and can be heated in order to ensure cleanness. A quadrupole mass spectrometer (Balzers QMS 112 A) is used to monitor the partial pressure of the reactive gases simultaneously during all experiments.

Figure 1 depicts a schematic sketch of the dielectric barrier discharge setup applied here. A sealed quartz glass tube with a wall thickness of 2.4 mm, filled with brass is used as isolated high voltage electrode. The Ge substrate forms the grounded counter electrode. An alternating high voltage pulse generator (Ingenieurbüro Dr. Jürgen Klein) with a pulse duration of $t_p = 0.6$ μs and a pulse repetition rate of 10 kHz is connected to the dielectric isolated electrode. A discharge gap of about $d = 1$ mm is used. During the treatment of the Ge substrate a voltage of $U = 11$ kV (peak) is measured. The high voltage supply delivers a power of $P = 2$ W. The process gas used for plasma treatment is O_2 at a pressure of 200 hPa or air at atmospheric pressure (around 950 hPa). The increase of the sample temperature during the plasma treatment does not exceed 10 K.[37]

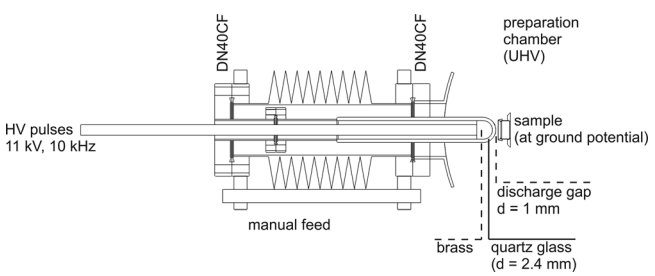

FIG. 1. Schematic drawing of the DBD alignment.

III. RESULTS AND DISCUSSION

The analysis of the data for the oxide surfaces requires fundamental knowledge of the spectroscopic results, especially for XPS. Therefore we start with the investigation of clean Ge(100) surfaces which will be the basis for the interpretation of the oxide surfaces.

A. Clean Ge(100) surfaces

The cleaning procedure is described in Sec. II. Figure 2(a) shows the XPS survey spectrum of a clean Ge(100) surface. We find the photoelectron peaks and Auger structures of germanium as well as a carbon peak due to a small contamination. Oxygen can barely be detected. We also find photoelectron peaks of molybdenum, originating in the sample holder. These peaks only have a small part in the spectrum, therefore they do not influence the interpretation of the measurements. The MIES and UPS spot sizes are small enough that no molybdenum is measured. We calculated a stoichiometry of 40.3% carbon, 52.3% germanium, and 7.4% oxygen.

Figures 2(b) and 2(c) display the XPS detail spectra of the O 1s and the Ge $2p_{3/2}$ peaks. The original data is plotted as black dots, the mathematical fit performed as described in Sec. II is displayed as a solid red line. The single Gaussians are shown as solid blue lines. A linear background correction is used. No assumptions have been made during the fitting procedure. In the O 1s region, a single small contribution is found. For Ge $2p_{3/2}$, we find a distinct peak at $E_B = 1218.1$ eV (denoted by I) which corresponds to non-oxidized Ge^0.[12,38] A small satellite peak at $E_B = 1220.2$ eV (peak II)

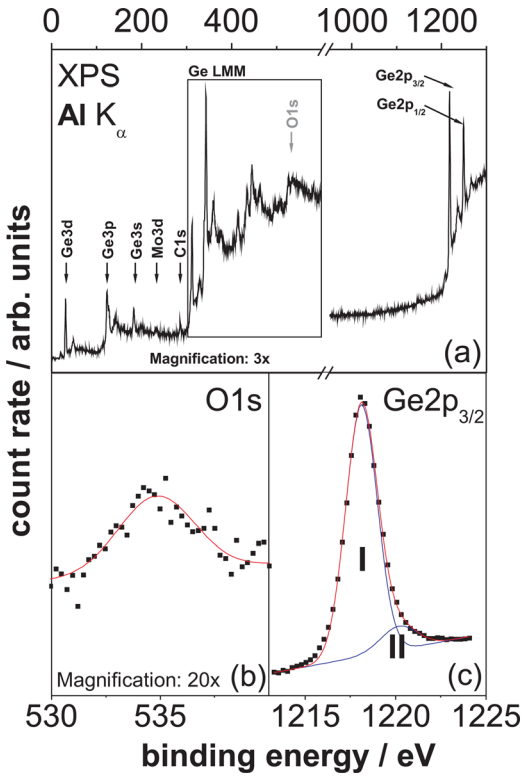

FIG. 2. (Color online) XPS survey (a) and detail spectra (O 1s (b) and Ge $2p_{3/2}$ (c) region) of the clean Ge(100) surface.

corresponds to a small contamination, most likely due to the observed carbon. The distance between these peaks is 2.1 eV and can be assigned to Ge^0 and Ge^{3+}.[11,12] The Ge^{3+} species holds a fraction of about 5% at the global stoichiometry. Together with the oxygen contribution of 7.4% this is consistent to Ge_2O_3. A shift of about 1 eV of the absolute binding energy relative to literature is observed for both of the Gaussian which could be due to Fermi level pinning at surface states and respective band bending. Other groups used more cycles of Ar^+ ion sputtering and thermal annealing,[39,40] as well as the cleaning procedure using ultraviolet-ozone and thermal annealing.[41] All XPS data are summarized in Table I for better comparison.

Figure 3 shows the MIES and UPS spectra of the clean Ge(100) surface. Due to the high work function of 4.6 eV no discrete peaks are visible in MIES. A broad structure appears at the low binding energy side of the secondary electron peak due to the AN process described in Sec. II. Even though the binding energy scale is only valid for the AD process, this spectrum has been displayed in the same manner as the other MIES spectra. Binding energies were calculated from kinetic energies by $E_B = 19.8\ \text{eV} - E_{kin}$ where 19.8 eV equals the binding energy difference of the He 1s and 2s orbitals. This AN spectrum fits well to comparable ones obtained for Ge(100) (Ref. 19) and Ge(111) surfaces.[18] AN spectra are composed by a self convolution of the SDOS mediated by a transition matrix element. In case that the AN process is possible, the competing AD process becomes less probable. Therefore, only AN is visible in the spectrum. It is well known, that even small traces of adsorbed oxygen would inhibit the AN process and therefore change the MIES spectrum to AD structures, which would be visible very clearly, as for example during the oxidation of iron.[42] From these MIES results and from the XPS data in Fig. 2 we can conclude, that the Ge(100) surface is free from oxygen atoms. In UPS we find emission almost up to the Fermi level at $E_B = 0$. Even though the features are broadened compared to literature, we find emission at the valence band and surface state energies as was found in the literature.[25] Thus, the spectrum resembles previous studies.[9,11,12]

B. Plasma treatment in an oxygen atmosphere

The treatment is performed in the preparation chamber at a constant oxygen pressure of 200 hPa for 60 s. Afterwards

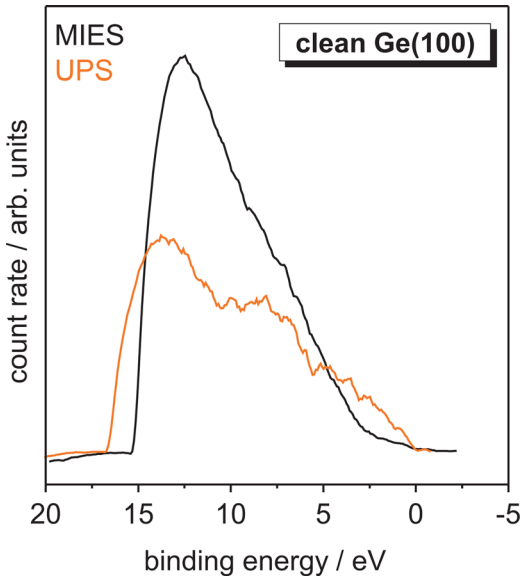

FIG. 3. (Color online) MIES and UPS spectra of a clean Ge(100) surface.

the preparation chamber is evacuated by opening the valves and starting the pumps with ongoing plasma treatment. It takes about 60 s to reach a pressure of 5×10^{-4} hPa where the plasma breaks down. It takes another 200 s at a further decreasing pressure to transfer the sample from the preparation chamber into the analysis chamber and to start the measurements.

Figure 4(a) shows a XPS survey spectrum of a Ge(100) surface after plasma treatment in an oxygen atmosphere. Only photoelectron and Auger peaks of germanium and oxygen are visible. Especially, no traces of carbon or any other contamination are detectable. The data yields a global stoichiometry of 23.4% germanium and 76.6% oxygen. Figure 4 also shows the XPS detail spectra of the O 1s (b) and the Ge $2p_{3/2}$ (c) peaks. The fitting was performed without using any constraints beforehand. For Ge $2p_{3/2}$ two species are visible. The first peak (I) has a binding energy of 1217.4 eV with a full width at half maximum (FWHM) of 2.1 eV and a fraction of about 3%. It can clearly be assigned to elemental germanium Ge^0 according to Sec. III A and Table I. The second peak (II) is located at a binding energy of 1220.5 eV with a FWHM of 2.5 eV. The energetic difference between this peak and the elemental peak Ge^0 amounts to 3.1 eV. It is

TABLE I. Summary of the XPS data of the Ge $2p_{3/2}$ and the O 1s region of the clean and plasma-treated Ge(100) surfaces.

		Ge $2p_{3/2}$			O 1s			
System	Peak	Binding energy in eV	FWHM in eV	Relative intensity	Binding energy in eV	FWHM in eV	Ratio O: Ge^{4+}	GeO_2- layer thickness in nm
Clean Ge(100) Fig. 2	I	1218.1	2.1	0.9				
	II	1220.2	2.4	0.1	—	—	—	—
Ge(100)O_2-plasma Fig. 4	I	1217.4	2.1	0.03				
	II	1220.5	2.5	0.97	532.2	2.5	3.37	3.6
Ge(100) air plasma Fig. 6	I	1217.9	2.2	0.07				
	II	1220.8	2.5	0.93	532.6	2.6	2.25	2.8

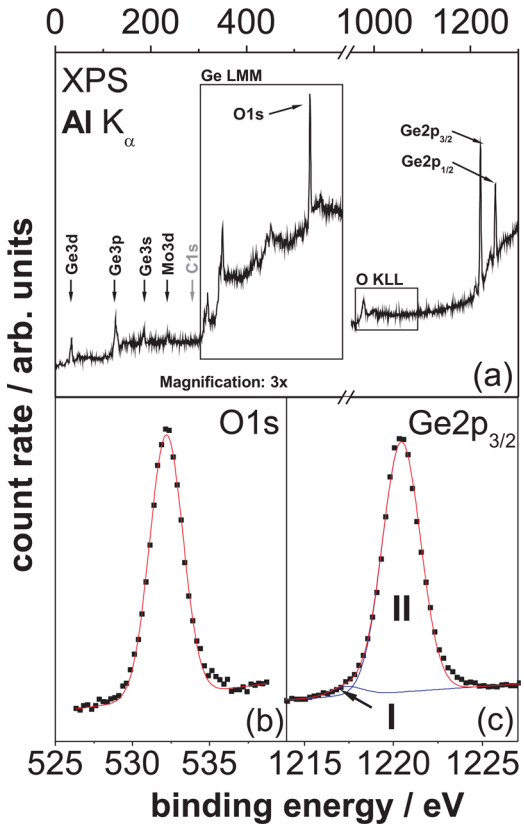

FIG. 4. (Color online) XPS survey spectrum (a) and detail spectra (O 1s (b) and Ge $2p_{3/2}$ (c) region) of the Ge(100) surface plasma-treated in 200 hPa of oxygen.

well known that the energetic difference between Ge^0 and Ge^{4+} is found between 2.9 and 3.2 eV.[9,11] Therefore the peak at 1220.5 eV must be interpreted as Ge^{4+}, thus representing GeO_2. The thickness of the oxide layer d is calculated by[17,21,23,43]

$$d = \lambda_o \cos\theta \ln\left[\left(\frac{D_m\lambda_m}{D_o\lambda_o}\right)\left(\frac{I_o}{I_m}\right)+1\right]$$

which results in a thickness of 3.6 nm. In the formula noted above, D_m and D_o are the atomic densities of germanium atoms in the substrate and in the oxide layer, λ_m and λ_o denote the corresponding inelastic mean free paths of the electrons and θ (10°) is the angle between the surface normal of the sample and the direction of the emitted electrons. The measured peak intensities of Ge^0 and Ge^{4+} are taken into account as I_m and I_o, respectively. The detail spectrum of the O 1s region shows only one peak at a binding energy of 532.2 eV with a FWHM of 2.5 eV.

Figure 5 shows the MIES and UPS spectra of the oxygen plasma treated Ge(100) surface. UPS shows a main peak at a binding energy of $E_B = 6.3$ eV, weak shoulders at $E_B = 8.2$ and 10.2 eV and a small contribution around $E_B = 3.6$ eV. The UPS spectrum resembles comparable ones from the literature well.[9,11,12] MIES in contrast shows only one distinct broad peak at $E_B = 7.8$ eV and weak contributions between $E_B = 3.5$ and 5.5 eV that might originate from physisorbed oxygen. In contrast to the clean Ge(100) surface an AD spectrum is observed. No MIES spectra for GeO_2 or other Ge

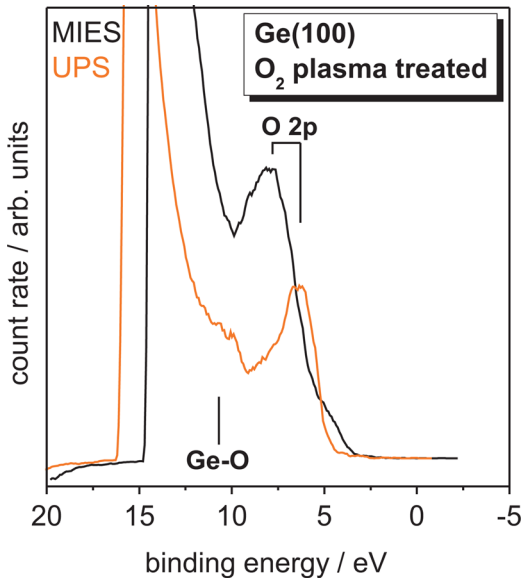

FIG. 5. (Color online) MIES and UPS spectra of the Ge(100) surface plasma-treated in 200 hPa of oxygen.

oxides are available from the literature for comparison. On SiO_2 surfaces in MIES and UPS comparable structures were found with a distinct MIES peak also at $E_B = 7.8$ eV.[44,45] This peak has the same origin like the UPS peak at $E_B = 6.3$ eV. It was interpreted to be due to non-bonding O 2p orbitals. The UPS structures at higher binding energies, which are not visible with MIES at all, correspond to a σ-type Si–O–Si bond. We assume that on Ge surfaces the electronic structures might behave comparably. The work function amounts to 5.2 eV for both MIES and UPS. No significant gap states can be observed. The binding energy difference for O 2p emission between MIES and UPS of about 1.5 eV might indicate band bending.[12]

C. Plasma treatment in air

The treatment is performed in the preparation chamber at a constant ambient air pressure of around 950 hPa for 60 s. Again, the preparation chamber was evacuated afterwards and the plasma was stable down to a pressure of 5×10^{-4} hPa which was reached about 60 s later. Sample transfer was done as described in Sec. III B.

Figure 6(a) shows the XPS survey spectrum of a Ge(100) surface after plasma treatment in air. As has been found for the treatment in pure oxygen described above only photoelectron and Auger peaks of germanium and oxygen are visible. Surprisingly, no traces of carbon, nitrogen or any other ambient air gas component are detectable. The data yields a stoichiometry of 32.4% germanium and 67.6% oxygen. The absence of nitrogen after the plasma treatment can be explained by the low substrate temperature[46] and the dominance of nitrogen radicals compared to nitrogen ions within the high pressure dielectric barrier discharge. Studies indicate that high pressure nitrogen plasma techniques generally lead to lower nitrogen surface concentrations compared to low pressure plasma treatments like electron cyclotron resonance or radial line slot antenna plasma.[46] In low

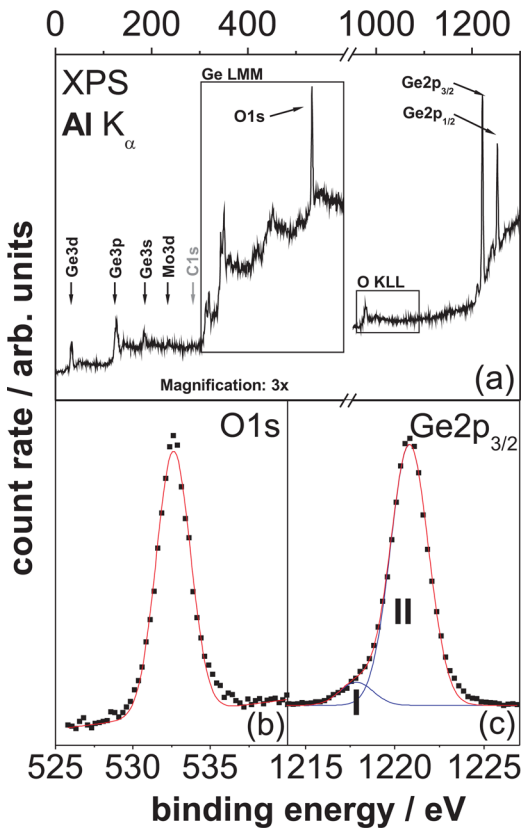

FIG. 6. (Color online) XPS survey spectrum (a) and detail spectra (O 1s (b) and Ge $2p_{3/2}$ (c) region) of the Ge(100) surface plasma-treated in 950 hPa of ambient air.

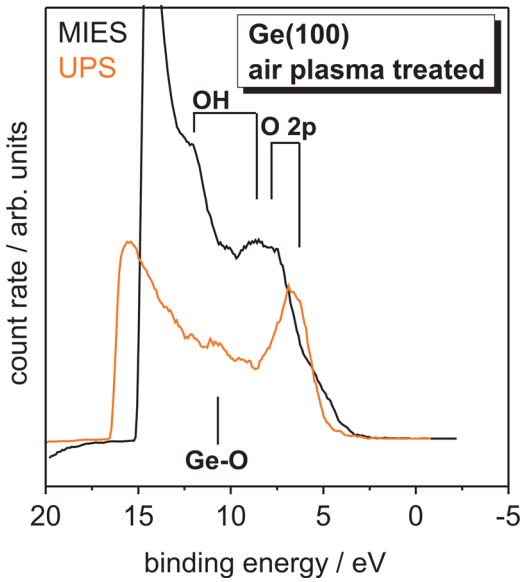

FIG. 7. (Color online) MIES and UPS spectra of the Ge(100) surface plasma-treated in 950 hPa of ambient air.

pressure plasma (typical pressures of less than 1 hPa) mainly nitrogen ions are found as reactive species.[47] These can be incorporated into the substrate by ion bombardment already at room temperature.[48] Nevertheless, we do not see any nitrogen in the plasma treated surfaces. This points out that the smaller amount of oxygen is not only sufficient to oxidize the surface but also to etch all nitride species.

Figures 6(b) and 6(c) display the XPS detail spectra of the O 1s and the Ge $2p_{3/2}$ peaks. As already described in Secs. III A and III B, no constraints have been used during the fitting procedure. Again, we observe two species for Ge $2p_{3/2}$. The first one at a binding energy of 1217.9 eV with a FWHM of 2.2 eV and a fraction of about 7% is due to elemental germanium. The second one at a binding energy of 1220.8 eV with a FWHM of 2.5 eV represents Ge^{4+} which means that even under these circumstances pure GeO_2 was formed. This claim is confirmed by the accordance of chemical shift and FWHM with Ge^{4+} in Sec. III B. The thickness of the oxide layer, estimated as described in Sec. III B, amounts to 2.8 nm. For the O 1s region, only one peak can be found at a binding energy of 532.6 eV with a FWHM of 2.6 eV.

Figure 7 shows the MIES and UPS spectra of the air plasma treated Ge(100) surface. In UPS the results are quite comparable to the ones obtained during plasma treatment in oxygen (see Fig. 5). MIES in contrast shows differences: we find additional structures at $E_B = 8.4$ eV and 12.0 eV. This doublet is well known from MIES spectra of OH terminated surfaces, for example $Ca(OH)_2$.[49] The fact that UPS barely shows these features implies that the OH groups are restricted to the top surface layer, where MIES is significantly more sensitive than UPS and XPS. The work function amounts to 4.8 eV for both MIES and UPS. Again, no significant gap states are found, whereas a binding energy difference for O 2p emission between MIES and UPS of 1.5 eV might indicate band bending.[12]

D. Comparison

We applied similar conditions for O_2 and atmospheric air plasma treatment at room temperature. The duration of 60 s, all plasma parameters and the oxygen partial pressure of 200 hPa are the same in both cases. We find oxide thicknesses of 3.6 nm for oxide and 2.8 nm for ambient atmosphere plasma.

The GeO_2 films appear to be well defined in both atmospheres, no traces of carbon or nitrogen atoms are found. Nevertheless, we find that the oxygen plasma film is over-stoichiometric compared to the atmospheric plasma film, the relative O 1s: Ge^{4+} ratios are 3.37 and 2.25, respectively. Surprisingly, we do not find any difference in the O 1s peaks energetic positions and FHWMs. This means that the oxygen must be incorporated without disturbing the chemical composition. It is known for amorphous SiO_2 that oxygen may be incorporated over-stoichiometrically.[50,51] We assume that a similar behavior takes place here which would hint at an amorphous GeO_2 layer. Under atmospheric conditions the excess supply of oxygen atoms may be reduced by the nitrogen atoms thus resulting in a near-stoichiometric composition of the GeO_2 film. On naturally oxidized Ge surfaces, we find a GeO_2 layer with a thickness of 0.93 nm and a O 1s: Ge^{4+} ratio of 2.15 (the XPS spectrum is not shown here). This is very close to the value for the atmospheric plasma.

IV. SUMMARY

The application of a DBD plasma treatment of Ge surfaces was performed under ambient atmospheric conditions and in an O_2 atmosphere with 200 hPa at room temperature. Under both conditions GeO_2 films were formed with thicknesses of 3.6 nm for O_2 and 2.8 nm for the ambient atmosphere. These films were built up within 60 s. All surfaces were prepared applying a standard cleaning procedure before treatment. The new procedure described here is much easier than most others presently applied in Ge technological applications. There is no need for reduced pressures, elevated temperatures, or sophisticated cleaning procedures.

[1]A. Delabie, F. Bellenger, M. Houssa, T. Conard, S. Van Elshocht, M. Caymax, M. Heyns, and M. Meuris, Appl. Phys. Lett. **91**, 082904 (2007).
[2]M. Kobayashi, G. Thareja, M. Ishibashi, Y. Sun, P. Griffin, J. McVittie, P. Piametta, K. Saraswat, and Y. Nishi, J. Appl. Phys. **106**, 104117 (2009).
[3]Y. Fukuda, K. Kato, H. Toyota, T. Ono, Y. Nagasato, and T. Ueno, Jpn. J. Appl. Phys. **45**, 7351 (2006).
[4]F. Bellenger, M. Houssa, A. Delabie, A. Afanasiev, T. Conrad, M. Caymax, M. Meuris, K. De Meyer, and M. M. Heyns, J. Electrochem. Soc. **155**, G33 (2008).
[5]L. Surnev, Surf. Sci. **110**, 439 (1981).
[6]J. Sládková, Czech. J. Phys. B **27**, 943 (1977).
[7]A. J. Mayne, F. Rose, and G. Dujardin, Surf. Sci. **523**, 157 (2003).
[8]D. Morkes, M. Ondrjcek, I. Ulrych, Z. Choj, H. Cobrad, and V. Cháb, Surf. Sci. **352**, 607 (1996).
[9]H. J. Kuhr and W. Ranke, Surf. Sci. **201**, 408 (1988).
[10]T. J. Grassman, S. R. Bishop, and A. C. Kummel, Surf. Sci. **602**, 2373 (2008).
[11]D. Schmeisser, A. Bogen, F. J. Himpsel, D. Rieger, G. Landgren, and J. F. Morar, Surf. Sci. **172**, 455 (1988).
[12]K. Prabhakaran, and T. Ogino, Surf. Sci. **325**, 263 (1995).
[13]J. M. Soon, C. W. Lim, K. P. Loh, N. L. Ma and P. Wu, Phys. Rev. B **72**, 115343 (2005).
[14]N. A. Tabet, M. A. Salim, and A. L. Al-Oteibi, J. Electron. Spectrosc. Relat. Phenom. **101–103**, 233 (1999).
[15]R. F. Lever and H. R. Wendt, Surf. Sci. **19**, 435 (1970).
[16]C. A. Carosella and J. Comas, Surf. Sci. **15**, 303 (1969).
[17]T. Deegan and G. Hughes, Appl. Surf. Sci. **123**, 66 (1998).
[18]S. Nannarone and L. Pasquali, Nucl. Instrum. Methods Phys. Res. B **182**, 227 (1991).
[19]S. Nishigaki, K. Yamada, M. Naitoh, and H. Iga, Surf. Sci. **363**, 121 (1996).
[20]H. Matsubara, T. Sasada, M. Takenaka, and S. Takagi, Appl. Phys. Lett. **93**, 032104 (2008).
[21]R. Das, M. K. Bera, S. Chakraboty, S. Saha, J. F. Woitok, and C. K. Maiti, Appl. Surf. Sci. **253**, 1323 (2006).
[22]N. A. Tabet and M. A. Salim, Appl. Surf. Sci. **134**, 275 (1998).
[23]V. Craciun, I. W. Boyd, B. Hutton, and D. Williams, Appl. Phys. Lett. **75**, 1261 (1999).
[24]T. Sasada, Y. Nakatika, M. Takenaka, and S. Takagi, J. Appl. Phys. **106**, 073716 (2006).
[25]K. Prabhakaran and T. Ogino, Surf. Sci. **316**, 1031 (1994).
[26]S. Zhaoqi and L. Chunrong, Semicond. Sci. Technol. **8**, 1779 (1993).
[27]M. Frerichs, F. Voigts, and W. Maus-Friedrichs, Appl. Surf. Sci. **253**, 950 (2006).
[28]J. H. Scofield, J. Electron Spectrosc. Relat. Phenom. **8**, 129 (1976).
[29]R. F. Reilman, A. Msezane and S. T. Manson, J. Electron. Spectrosc. Relat. Phenom. **8**, 389 (1976).
[30]C. Powell and A. Jablonski, J. Electron. Spectrosc. Relat. Phenom. **178**, 331 (2010).
[31]National Institute of Standards and Technology Electron Inelastic-Mean-Free-Path Database 1.1, http://www.nist.gov/srd/nist71.cfm (visited: 18 May 2011).
[32]Y. Harada, S. Masuda, and H. Ozaki, Chem. Rev. **97**, 1897 (1997).
[33]H. Morgner, Adv. At., Mol., Opt. Phys. **42**, 387 (2000).
[34]G. Ertl and J. Küppers, *Low Energy Electrons and Surface Chemistry* (VCH Verlag, Weinheim, 1985).
[35]M. Frerichs, F. X. Schweiger, F. Voigts, S. Rudenkiy, W. Maus-Friedrichs, and V. Kempter, Surf. Interface Anal. **37**, 633 (2005).
[36]M. Frerichs, F. Voigts, S. Hollunder, R. Masendorf, A. Esderts, and W. Maus-Friedrichs, Appl. Surf. Sci. **252**, 108 (2005).
[37]U. Kogelschatz, Plasma Chem. Plasma Phys. **23**, 1 (2003).
[38]B. Pelissier, H. Kambara, and O. Joubert, Microelectron. Eng. **85**, 151 (2008).
[39]A. Molle, N. K. Bhuiyan, G. Tallarida, and M. Fanciulli, Appl. Phys. Lett. **89**, 083504 (2006).
[40]L. H. Chan, E. I. Altman, and Y. Liang, J. Vac. Sci. Technol. A **19**, 976 (2001).
[41]X.-J. Zhang, A. Agarwal, R. Tsu, M.-A. Hasan, J. E. Greene, and A. Rockett, J. Vac. Sci. Technol. A **11**, 2553 (1993).
[42]K. Volgmann, F. Voigts, and W. Maus-Friedrichs, Surf. Sci. **604**, 906 (2010).
[43]B. Strohmeier, Surf. Interface Anal. **15**, 51 (1990).
[44]M. Brause, B. Braun, D. Ochs, W. Maus-Friedrichs, and V. Kempter, Surf. Sci. **398**, 184 (1998).
[45]M. Brause, D. Ochs, Th. Mayer, B. Braun, V. Puchin, W. Maus-Friedrichs, and V. Kempter, Surf. Sci. **383**, 216 (1997).
[46]T. Sugawara, R. Sreenivasan, and P. C. McIntyre, J. Vac. Sci. Technol. B **24**, 2442 (2006).
[47]M. Mukhopadhyay, S. K. Ray, and C. K. Maiti, J. Vac. Sci. Technol. B **1**, 1682 (1996).
[48]D. Aubel, M. Diani, and D. Bolmont, J. Non-Cryst. Solids **187**, 319 (1995).
[49]F. Bebensee, F. Voigts, and W. Maus-Friedrichs, Surf. Sci. **602**, 1622 (2008).
[50]D.-Q. Yang, M. Meunier, and E. Sacher, J. Appl. Phys. **99**, 084315 (2006).
[51]L. Galán, I. Montero, F. Rueda, and J. M. Albella, Surf. Interface Anal. **19**, 473 (1992).